SIMULATION STUDY ON PARAMETRIC MODELLING OF MAGNETORHEOLOGICAL DAMPER SYSTEM

Ismail Mohammad Sabri, Mat Hussin Ab Talib*

Faculty of Mechanical Engineering, Universiti Teknologi Malaysia, 81310 UTM Johor Bahru, Johor, Malaysia

*Corresponding email: mathussin@utm.my

Article history
Received
1st November 2023
Revised
14th January 2024
Accepted
6th February 2024
Published
17th June 2024

ABSTRACT

The Magnetorheological (MR) damper system serves as a semi-active suspension system designed to absorb road disturbances. This research aims to replicate the MR damper system through a parametric modeling approach, specifically employing the Simple Bouc-Wen Model, Spencer Model, and Hyperbolic-Tangent Model. The objective of this paper is to assess the effectiveness of these modeled MR damper systems with the utilization of a Fuzzy-PID controller. The simulation process is conducted within MATLAB Simulink, whereby a block diagram is devised based on equations related to the suspension system and the parametric models. The inputs for the system encompass sinusoidal and bump road profiles. The outcomes from the modeled MR damper systems reveal that the semi-active suspension system outperforms the passive suspension system. The primary simulation metrics under consideration include sprung displacement, sprung acceleration, and unsprung acceleration. Among the three MR damper models, the Hyperbolic-tangent model displays the most favorable performance, with a mean squared error of 51.44%, while the Bouc-Wen model exhibits the least favorable performance, registering a mean squared error of 25.96%. The integration of the Fuzzy-PID controller demonstrates an enhancement in the sprung suspension system, though the sprung acceleration remains relatively unchanged.

Keywords: *MR damper, Bouc-Wen, Spencer, Hyperbolic-tangent, Fuzzy-PID*

1.0 INTRODUCTION

The Magnetorheological (MR) damper system finds widespread application in various industries, particularly within the automotive sector. This damper system has gained significant popularity, being employed in high-end vehicles like Ferrari, Audi, Ford, and others. An MR damper is essentially a shock absorber containing MR fluid, and its behavior is controlled through electromagnets. Typically, MR dampers are closely associated with semi-active suspension systems, with their inception dating back to the early 1970s [1]. These MR dampers are predominantly utilized in vehicle suspension systems, structural vibration control, and even as shock absorbers in space shuttles, among other applications. Given the increasing emphasis on ride comfort in the automotive industry, suspension systems have become a focal point. When driving on rough and uneven roads with potholes, vehicles require a swift response to effectively counter vibrations [2-3]

In this research endeavor, an exploration of the MR damper system is conducted through the application of diverse parametric modeling approaches. It is anticipated that these distinct parametric models will yield varying outcomes pertaining to the

characteristics of the MR damper. Given the extensive body of research dedicated to elucidating the features of MR damper systems, this study introduces a novel element by incorporating the application of a Fuzzy-PID controller within these MR damper systems. Numerous prior studies have corroborated the efficacy of Fuzzy-PID controllers in managing intricate and imprecise non-linear models [4-5].By employing the Fuzzy-PID controller in this study, a comparative analysis of the obtained results can be conducted. It is reasonable to assume that the results will reveal more precise behavioral characteristics of the MR damper system when compared to a MR damper system that does not utilize the Fuzzy-PID controller. In the past, automotive suspension design primarily focused on ensuring passenger comfort and vehicle stability during motion. The suspension system was designed to bear the vehicle's weight, provide passenger isolation, and distribute the loads generated by road disturbances [6-7]. The suspension system functions by storing energy using springs and dissipating it through dampers. The key distinction between passive suspension systems and semi-active suspension systems lies in the parameter behaviour. In passive suspension systems, parameters remain constant, leading to suboptimal damping values when encountering different road profiles because the damper's value is fixed and determined by the number of holes on the cylinder piston. Moreover, passive suspension systems are slower to respond when subjected to maximum force during sharp cornering. While active suspension systems exist, they are prohibitively expensive [8-9]. As a response to these challenges, the concept of semi-active suspension emerged from the engineering community. A semi-active suspension system allows the damping coefficient to be adjusted based on the prevailing road conditions. In this scenario, the magnetorheological (MR) damper takes the place of the traditional damper in the semi-active suspension system. Nevertheless, forecasting the behavior of the MR damper proves to be a challenging endeavor due to its non-linearity and hysteresis. Consequently, scholars and engineers have developed mathematical models aimed at forecasting the MR damper's characteristics.

This paper is organised as follows: The passive and semi-active suspension damper models are explained in Section 2, and Section 3 introduces the Fuzzy-PID controller algorithms. In section 4, simulation analysis will be discussed utilising the proposed controllers to model and control the suspension system. The broad conclusions are presented in section 5.

2.0 SUSPENSION SYSTEM MODELLING

2.1 Passive suspension system

The passive suspension system consists of spring and damper. Both structures will be installed in parallel position to support the sprung mass. Then, the second spring will be placed at the unsprung mass. The unsprung mass is located between road surface and wheel. The parameters of the passive suspension system are constant. The spring constant and damper constant are suitable to be used for passenger’s comfort. For this project, the focus will be on quarter-car model with two degree of freedom (2-DOF). The interest in this modelling is to find the behavior of the suspension system. Figure 1 is the model for passive suspension system.

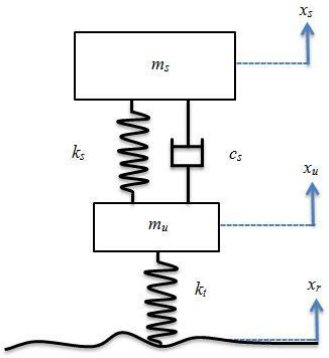

Figure 1: Model of Passive Suspension System

Based on the model of passive suspension, the equation is abstracted based on Newton's Second Law. The equation is as below:

For Sprung Mass, m_s

$$m_s\ddot{x}_s = k_t(x_t - x_s) + c_s(\dot{x}_u - \dot{x}_S) \quad (1)$$

For Unsprung Mass, m_u

$$m_u\ddot{x}_u = k_t(x_r - x_u) - k_s(x_u - x_s) - c_s(\dot{x}_u - \dot{x}_s) \quad (2)$$

In relation to Equations (1) and (2), some parameters have been sourced from prior research [10]. The model is constructed within the MATLAB Simulink block, and all the parameters are essential for the model's completion. Specific values for these parameters are outlined in Table 1. The completed block diagram for the model is also shown in Figure 2.

Table 1: Quarter vehicle suspension parameters

Parameter	Value (unit)
M_s	240 (kg)
M_u	36 (kg)
K_s	16 (kN/m)
K_u	160 (kN/m)
C_s	980 (Ns/m)

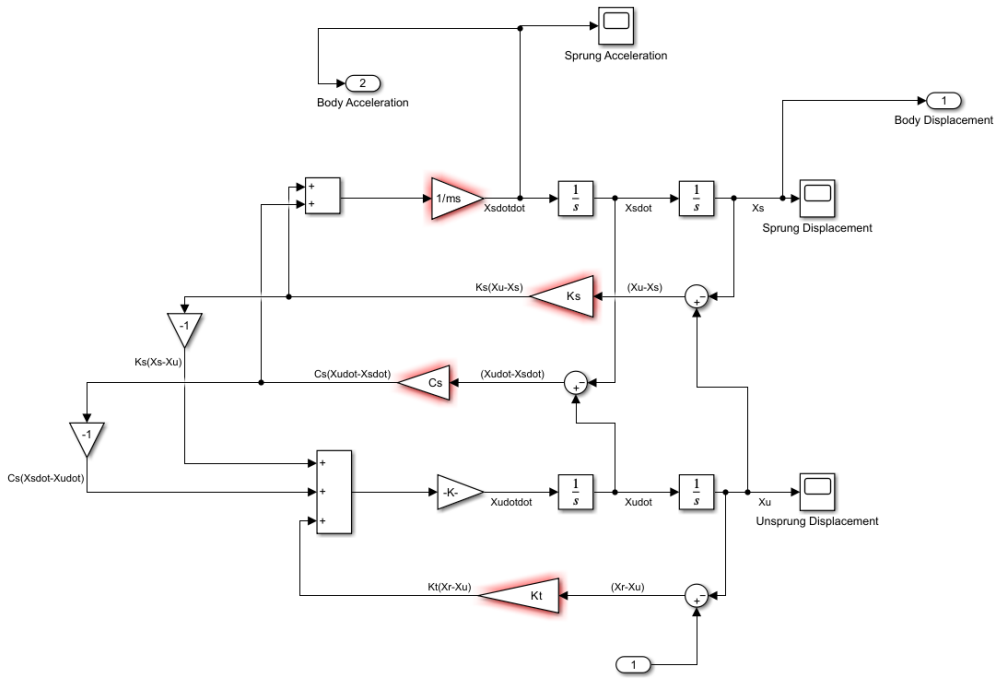

Figure 2: Modelling of passive suspension system

According to the Figure 2, the road profile is set by the signal generator with 0.01m for the amplitude with 5 Hz frequency. Based on the passive suspension system developed for sprung and unsprung masses, the natural frequency has been identified. The natural frequency obtained is in the range between 8.26 Hz to 69.6 Hz respectively for sprung and unsprung masses. It is possible to identify an appropriate road profile input for the system using the data obtained.

2.2 Semi-active suspension system

Semi-active suspension systems are mathematically modelled differently from passive suspension systems. Figure 3 shows the derivation of m_u (unsprung mass) and m_s (sprung mass)

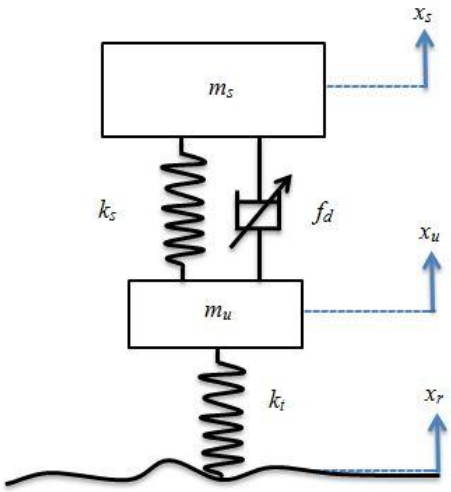

Figure 3: Quarter car semi-active suspension system

Based on the Figure 3, the equation that can be extracted are as follow:

For m_u,
$$m_u\ddot{x}_u = k_t(x_u - x_r) - k_s(x_u - x_s) - c_s(\dot{x}_u - \dot{x}_s) - f \quad (3)$$

For m_s,
$$m_s\ddot{x}_s = k_s(x_s - x_u) - c_s(\dot{x}_S - \dot{x}_u) - f \quad (4)$$

2.3 Bouc-Wen Model

A high accuracy and traceable model are needed to activate the MR damper's ability to be controlled due to its high non-linearity and hysteretic. To describe the nonlinear behaviour of MR dampers, a few parametric mechanical models have been developed. One of the most successful models is the Simple Bouc-Wen Model that appropriately predict MR damper behaviour and stimulates its ability to operate as a semi-active controller [11-12]. Figure 4 has shown the simple model of Bouc-Wen to trace the behaviour of MR damper.

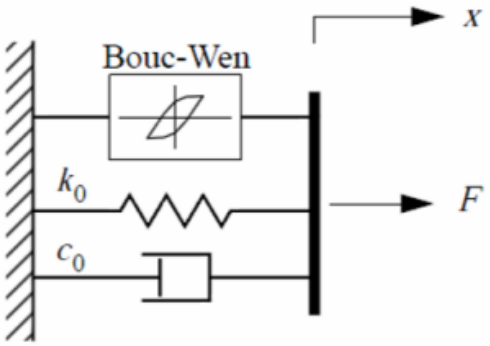

Figure 4: Schematic diagram of Simple Bouc-Wen Model

From Figure 4, the equation from Bouc-Wen model can calculate the non-linear force as follows:

$$F = az + c_o\dot{x} \quad (5)$$

where a is the Bouc-Wen model parameter related to the yield stress. Meanwhile, c_o is the dashpot damping coefficient as shown in Figure 5:

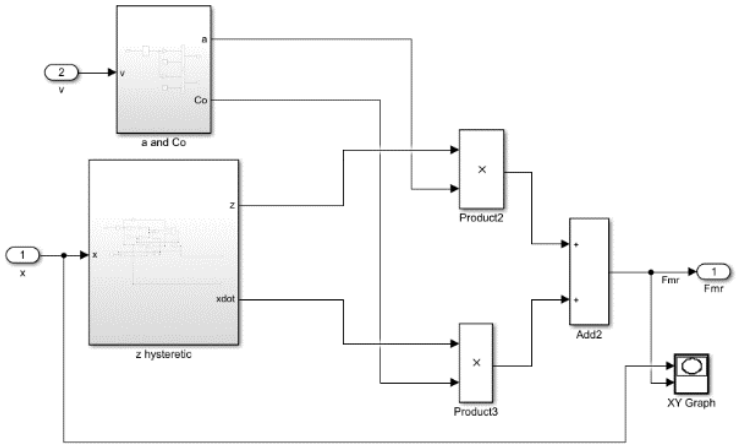

Figure 2.5: Magnetorheological Force equation

z is the parameter that will trace the hysteretic deformation which defined by the following equation:

$$\dot{z} = -\gamma|\dot{x}|z||\dot{z}|^{n-1} - \beta\dot{x}|z|^n + A\dot{x} \quad (6)$$

in which A, β and γ are the Bouc-Wen model parameters.

In order a control system equipped with MR dampers may work at its optimal level, its voltage must be able to be altered so that damping force can be changed based on the measurement of feedback at any given time. Accordingly, the requirement can be addressed by modifying linearity of parameters A, β, γ and n under unloading conditions, as well as smoothness of transitions from the pre-yield to post-yield region. The command voltage, u, to the current driver that will manipulate the parameters of model is as Equation 7:

$$\alpha = \alpha_a + \alpha_b u, and\ c_0 = c_{0a} + c_{0b} u \quad (7)$$

2.4 Spencer Model

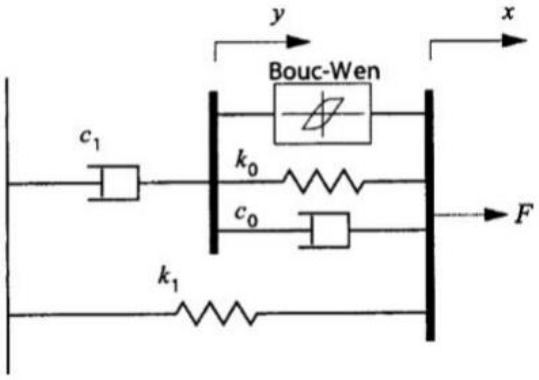

Figure 6: Spencer Model

The Spencer Model has been adjusted and modified by Spencer as shown as in Figure 6. Due to extra parameters as input, this model seems to predict accurately the behaviour of MR damper [13]. Equation 2.8 is used to govern the force prediction:

$$F(t) = az + c_0(\dot{x} - \dot{y}) + k_0(x - y) + k_1(x - x_0) = c_1\dot{y} + k_1(x - x_0) \quad (8)$$

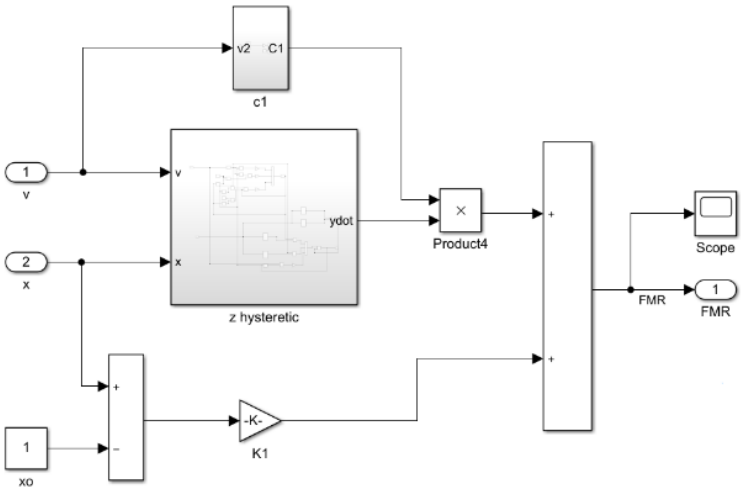

Figure 7: Magnetorheological Force equation

where *x* is the displacement of the damper, and the evolutionary variable *z* is governed by:

$$\dot{z} = -\gamma|\dot{x} - \dot{y}||z|^{n-1}z - \beta(\dot{x} - \dot{y})|z|^{n} + \delta(\dot{x} - \dot{y}) \quad (9)$$

and

$$\dot{y} = \frac{1}{(c+c_1)}[\alpha z + k_0(x - y) + C_0\dot{x}] \quad (10)$$

Just like the previous model, the command voltage, *u*, to the current driver will be dependent by the following parameters:

$$\alpha = \alpha(u) = \alpha_a + \alpha_b u, c_0 = c_0(u) = c_{1a} + c_{1b}u\, c_1 = c_1(u) = c_{1a} + c_{1b}u \quad (11)$$

It is also necessary to consider the dynamics involved in MR fluid acquiring the rheological fluid equilibrium in addition to the filtration of first order

$$\dot{u} = -\mu(u - v) \quad (12)$$

where *v* is a command voltage applied to the current driver.

2.5 Hyperbolic Tangent Model

Hyperbolic Tangent model will be applied to accurately predict the hysteretic and linear functions, as well as to describe viscosity and stiffness, in hyperbolic tangent function. The equation of this model is given by:

$$f = c\dot{x} + kx + \alpha z + f_o \quad (13)$$

$$z = tanh\big(\beta\dot{x} + \delta\, sign(x)\big) \quad (14)$$

where x and $\dot{x}$ would be the displacement and velocity, respectively, of the piston of MR damper; *c* and *k* would be the viscous coefficient and stiffness of spring, respectively; α is the scale factor of the hysteretic of model; β and δ are the parameters that controlling the shape of the hysteretic loops; and f_o is the damper force offset.

Based on the equation, the hyperbolic tangent model has only simple function, which makes it easy to identify and compute. MR damper hysteretic and linear function can be expressed using this model. However, this approach requires the identification of six parameters and a complicated mathematical theorem. Five parameters have been found in order to simplify the model, and the equation that will control the modified model is presented as follows:

$$f = a_1 \tanh\big(a_2(\dot{x} + kx)\big) + a_3(\dot{x} + kx) + f_0 \quad (15)$$

where a_1 is a scale factor of the hysteresis, which is related to the control current; a_2 and a_3 are the parameters related to the viscous damping coefficient in the pre-yield region to post-yield region, respectively; and $k = V_0/X_0$, V_0 and X_0 are define as the absolute value of the critical piston velocity and critical piston displacement when the damping force, f, is zero, respectively), which is a scale factor of hysteresis loop width [14].

According to the experiment conducted by the [5], the value of a_2, *k*, and f_0, are not contributing to significant difference under different influence of currents, which mean, these three parameters can be considered as constant value and the values are a_2 = 776.5809, *k* = 0.3506, and f_0 = 7.1671. As a result, they believe that as the value of current

grows, the a_1 and a_3 will also increase, which can be explained by the linear relationship between the two. Hence, these can be obtained by linear progression approach, and it is expressed as Equation 16

$$a_1 = b_1 I + c_1 \text{ and } a_3 = b_2 I + c_2 \quad (16)$$

where, b_1 is 117.2610, c_1 is 40.4957, b_2 is 484.3815 and c_2 is 167.2799.

Therefore, the final equation of Hyperbolic Tangent Model is given by:

$$f = (b_1 I + c_1)\, tanh\big(a_2(\dot{x} + kx)\big) + (b_1 I + c_1)(\dot{x} + kx) + fo \quad (17)$$

Equation 17 can use the function of SIMULINK to create the block as shown in Figure 8:

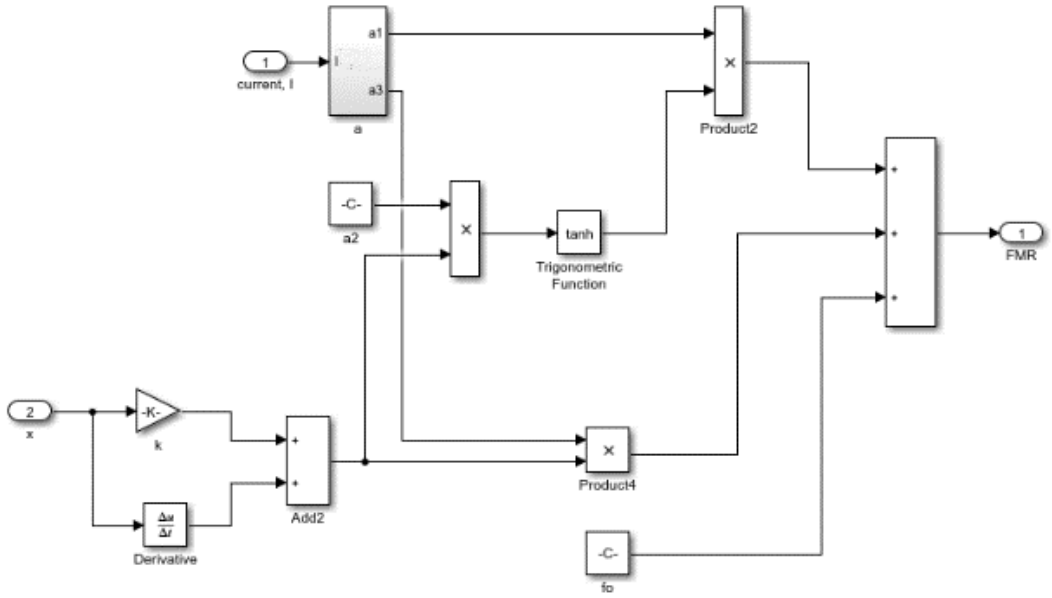

Figure 8: Magnetorheological Force of Hyperbolic-Tangent Function

2.6 Selection of the Parameters

The parameters as shown in Table 2 are extracted from [4] where these parameters have been tested for simulation purpose.

Table 2: Identified parameters of Simple Bouc-Wen and Spencer Model

Parameter	Unit	Bouc-Wen Model values	Spencer Model values
X_o	m	-	-
γ	m^{-2}	141	164
β	m^{-2}	141	164
A	-	2075	1107.2
n	-	2	2
a_a	kN/m	26	46.2
a_b	kN/m/V	29.1	41.2
c_{oa}	kN.s/m	105.4	110
c_{ob}	kN.s/m/V	131.6	114.3
c_{Ia}	kN.s/m	-	8359.2

c_{Ib}	kN.s/m/V	-	7482.9
k_o	kN/m	-	0.002
k_1	kN/m	-	0.0097
η	s^{-1}	100	100

3.0 FUZZY-PID CONTROLLER DESIGN

An accurate mathematical model is not required for the fuzzy controller to be effective, nor is it necessary for an experienced operator to apply the nonlinear control effect using his/her skills. These fuzzy controllers have been tested on a variety of active and semi-active suspension vibration control systems, with positive results. In addition, the Fuzzy-PID controller allows the system to receive the benefits of each of the controllers, resulting in a robust performance and higher adaptability to a lot of problems. In this project, the fuzzy will be used to tune the value gain of the PID controller.

This initial arrangement uses a fuzzy control system to manage the outer loop loops of the outer loop controller. In this project, two fuzzy inputs will be used. Unsprung displacement is one of the mistakes when comparing spring displacement to unsprung displacement. And the mistake's derivative is yet another input. An established PID controller's proportional, integration and differentiation properties can be stated in the following way:

$$u(t) = K_p e(t) + K_i \int_0^t e(t)\, dt + K_d \frac{de(t)}{d(t)} \tag{18}$$

where the K_p is the gain of proportional, K_i is gain of the integral and lastly K_d is the gain of differential. Then, *e(t)* is the error of the system which is the difference of the sprung and unsprung displacement, and *u(t)* is the desired damping force needed by the system. Since the Fuzzy-PID can automatically update the PID values based on fuzzy control theory, it may be used for many applications, combining fuzzy and PID controllers' strengths in terms of flexibility, robustness and simplicity. A high-dynamic and static performance system can benefit from this method by enhancing the system's dynamic response. Being a Fuzzy PID controller, the equation may be stated as follows:

$$u(t) = K_{p2} e(t) + K_{i2} \int_0^t e(t)\, dt + K_{d2} \frac{de(t)}{d(t)} \tag{19}$$

where, $K_{p2} = K_p * K_{p1}, K_{i2} = K_i * K_{i1}, K_{d2} = K_d * K_{d1}$ and K_{p1}, K_{i1}, K_{d1} are the gain output s from the fuzzy controller.

Fuzzy logic self-tuning of a PID controller with two inputs and three outputs is proposed in this study. The fuzzy self-tuning employed the error and rate of error as inputs and the gains as outputs in the controller design. Adding the Fuzzy to the PID controller allows the PID controller to adjust its parameters on-line based on the change in signal error and error change. As shown in Figure 9, the proposed controller also includes scaling gains inputs.

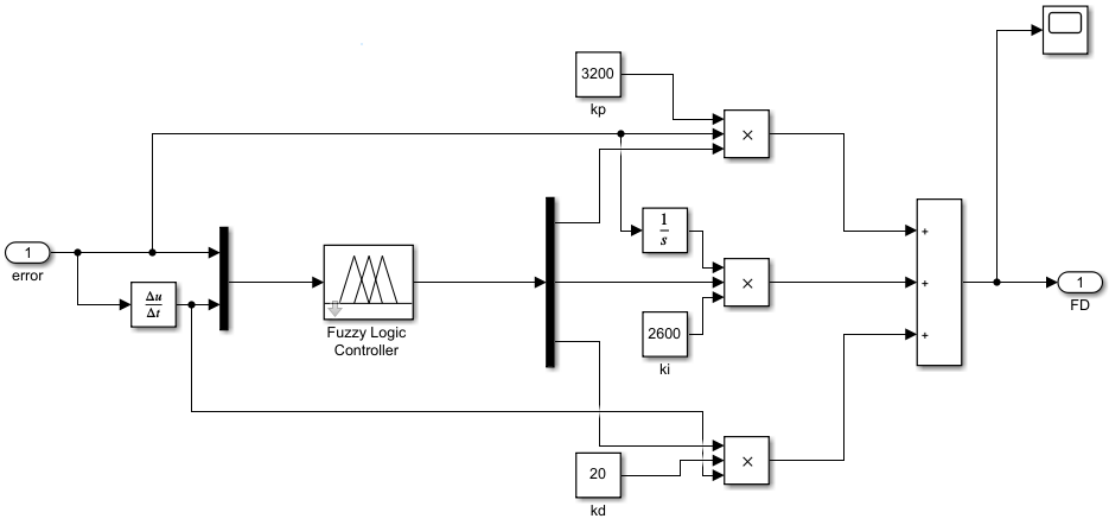

Figure 9: Block diagram of Fuzzy-PID Controller

4.0 RESULTS AND DISCUSSION

For the purpose of conducting an analysis and evaluating the efficacy of the MR damper models, it is essential to establish a road profile within the simulation. In this simulation, a sinusoidal waveform with an excitation amplitude of 0.001 and a frequency of 5 Hz is employed as the chosen road profile. Additionally, the simulation duration for each model is configured to be 1 second. Following the completion of parameter identification, which, for this simulation, involves referencing parameters from relevant journals to align with the objectives of this project, the subsequent analysis is based on the distinctive patterns generated by each model. This analysis serves the purpose of comparing the Bouc-Wen model, Spencer model, and Hyperbolic Tangent model.

4.1 Analysis on result of MR damper modelling

The analysis of the modelling of Bouc-Wen model and Spencer model are produced from different voltage values that are constant. The voltage started from 0,1,2,3 and 4 Volt. While for the Hyperbolic Tangent model, the current varies from 0A, 0.25A, 0.5A 0.75A, and 1A. The pattern of the results produced are as desired outcome. The Bouc-Wen and Spencer models obtain the desired outcome of the graphs' pattern when run with 0.05 of the amplitude but when the amplitude is lowered to 0.01, the pattern of the graph is off from the predicted output. However, the pattern of the graph seems steady and does not change much for Hyperbolic Tangent model regardless of the changing of amplitude. When the figures obtained from the modelling, the magnitude of the graph is to be analysed and the Bouc-Wen and Hyperbolic-Tangent model produced a pattern of graph that is decreasing in force over time while Spencer model is more to constant pattern. The Hyperbolic-Tangent model has produced the lowest force magnitude while Bouc-Wen model has produced the highest force magnitude across the damper. The results obtained from the proposed parametric models of MR damper can be referred to Figures 10 to 12

4.1.1 Bouc-Wen model

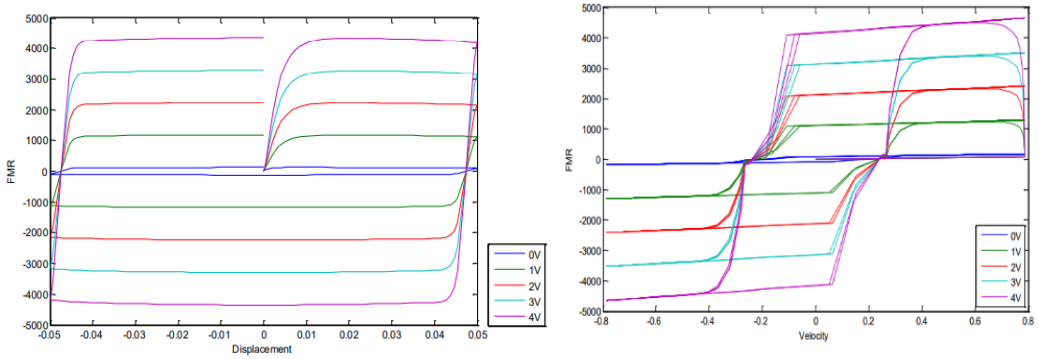

(a) (b)

Figure 10: Analysis for (a) Damper force vs displacement (b) Damper force vs velocity

4.1.2 Spencer model

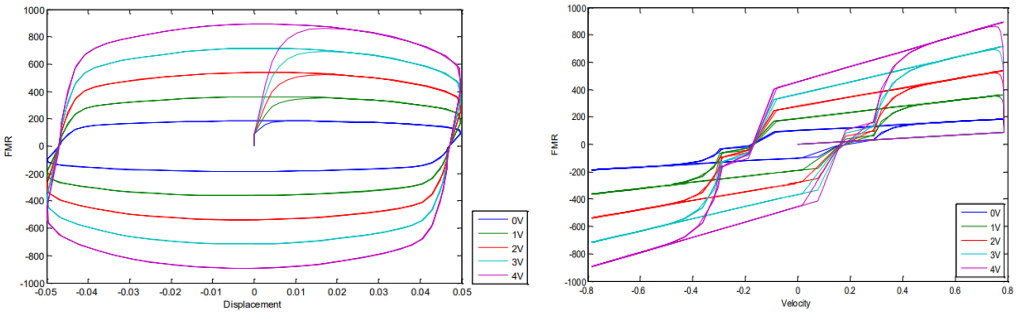

(a) (b)

Figure 11: Analysis for (a) Damper force vs displacement (b) Damper force vs velocity

4.1.3 Hyperbolic-Tangent model

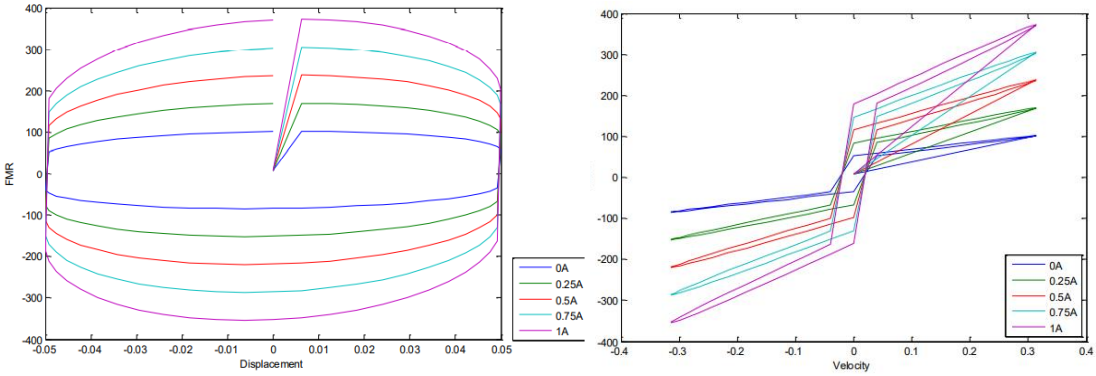

(a) (b)

Figure 12: Analysis for (a) Damper force vs displacement (b) Damper force vs velocity

4.2 Analysis on Fuzzy-PID Controller's Performance

The simulation in the MATLAB-Simulink for the MR damper use various types of mathematical model which require different tuning for PID values. The values for PID are manually tuned to obtain the desired output. Table 3 shows the PID parameters that have been used in the system:

Table 3: PID controller parameter

	Bouc-Wen Model	**Spencer Model**	**Hyperbolic-Tangent Model**
K_{p2}	3200	800	2800
K_{i2}	2300	300	100
K_{d2}	15	10	250

A comparison of semi-active and passive suspension systems showed that the sinusoidal road profile provided a better representation of the differences between the two systems. As compared to a passive suspension system, the semi-active suspension system's measured magnitude parameter shows a better improvement than a passive suspension system. After applying a disturbance, the semi-active suspension system's settling period has been considerably shortened.

The purpose of the modelled MR damper is to improve the suspension system in term of the sprung acceleration, suspension travel and tire acceleration. Table 4 shows the different in MSE values between passive and semi-active suspension system that have been achieved when running the simulation. From the data collected, the value of sprung acceleration and sprung displacement of Hyperbolic-Tangent model show that it has achieved an improvement in absorbing the road disturbance of about 50 % more than the passive suspension system. Detail of result is depicted in Figure 13.

Table 4 MSE with sinusoidal road profile

	PS	**BW**		**SP**		**HTM**	
	MSE	MSE	Red%	MSE	Red%	MSE	Red%
X_s	0.0135	0.0104	25.96	0.0102	27.67	0.0073	51.44
$\ddot{X}_s$	18.6322	13.2537	27.67	12.8947	29.55	8.8136	50.52
$\ddot{X}_u$	8.5221	20.9312	-60.15	8.1592	4.42	11.0422	-30.64

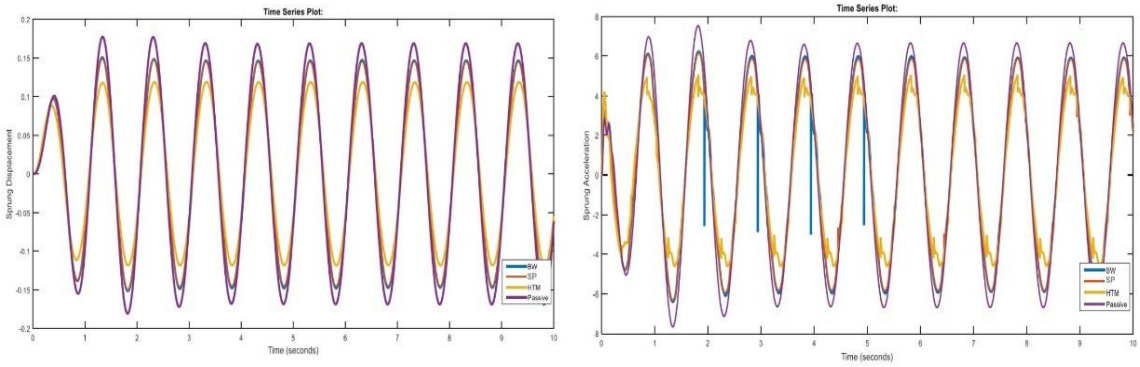

(a) (b)

Figure 13: Analysis for (a) Body displacement vs time (b) Body acceleration vs time

While using the data collected from bump road profile as in Table 5, semi-active suspension systems have a small improvement in MSE compared to passive suspension systems, but there is no gain in sprung acceleration and unsprung acceleration, according to the simulation. Since the primary goal of this simulation is to regulate the vehicle's acceleration, other output signals, such as suspension travel, may not increase the wheel displacement in time domains when random disturbances are introduced to a semi-active suspension system. Detail of result can be depicted in Figure 14.

Table 5 MSE with bump road profile

	PS	**BW**		**SP**		**HTM**	
	MSE	MSE	Red%	MSE	Red%	MSE	Red%
$X_s\,(x10^{-4})$	1.17	1.13	2.74	1.13	3.11	1.08	7.04
$\ddot{X}_s$	8.65	10.94	-26.36	10.69	-23.55	12.33	-42.30
$\ddot{X}_u\,(x10^{3})$	3.05	2.92	4.00	2.90	4.70	2.81	7.51

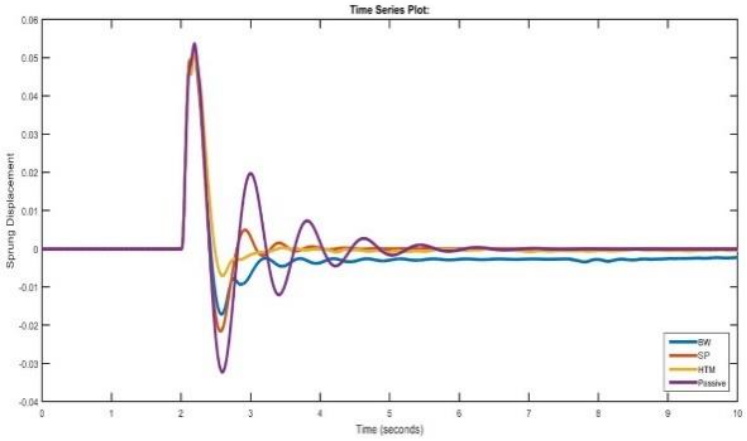

(a)

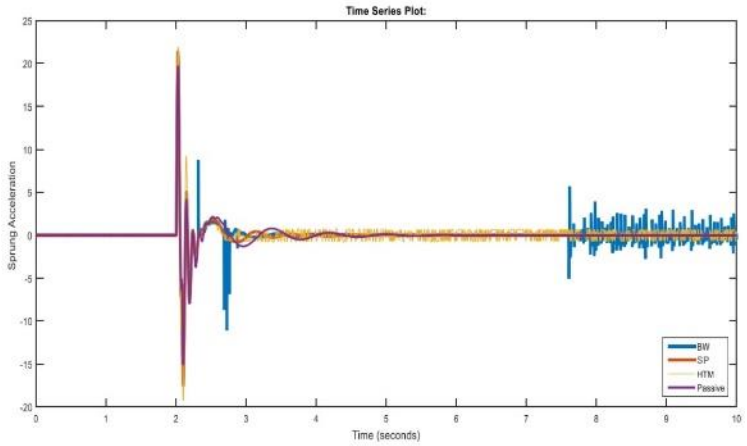

(b)

Figure 14: Analysis for (a) Body displacement vs time (b) Body acceleration vs time

Based on the road profiles currently in use, there appears to be an issue with the ability of various semi-active suspension system models to effectively adjust to different road disturbances. The problem arises when the damper cannot accurately gauge the required flexibility, especially when the absolute velocity of the vehicle body has a different

direction from the relative velocity. This issue is evident in simulations involving sinusoidal and bump road disturbances. In contrast to passive suspension systems, which take 6.5 seconds to stabilize, semi-active suspension systems demonstrate improved settling times. Specifically, the Bouc-Wen model, Spencer model, and Hyperbolic-Tangent model require only 5.3 seconds, 3.9 seconds, and 3.6 seconds, respectively, to settle. The voltage and current applied serve as inputs to the MR damper, while the Fuzzy-PID controller calculates the desired damping force. These inputs are derived from the suspension deflection and its rate of change, ensuring the production of the desired damping force. However, it's important to note that the damper is configured to apply minimal damping force only when the energy from the system dissipates from the MR damper.

5.0 CONCLUSION

The utilization of the Fuzzy-PID controller serves the purpose of enabling a wide range of controllable damping forces, particularly when encountering various types of road obstacles. With the controller in place, the study's goal is to evaluate the MR damper's performance, and the results demonstrate that the MR damper exhibits anticipated behavior. Notably, the modeled MR damper's performance is enhanced, characterized by reduced settling time and decreased amplitudes for sprung displacement, sprung acceleration, and unsprung acceleration compared to the passive suspension system. Among the three model types, the Hyperbolic-Tangent model showcases the highest performance, while the Bouc-Wen model exhibits the least, with the Spencer model falling in between. The performance of the MR damper system with Hybperbolic tangent model shows a better amplitude reduction in the form of the body acceleration and body displacement analysis with up to 51.44%.

ACKNOWLEDGEMENT

The authors would like to express their gratitude to Universiti Teknologi Malaysia (UTM) for funding and providing facilities to conduct this research

References

[1] Yao, G. Z., Yap, F. F., Chen, G., Li, W. H., and Yeo, S. H. *MR damper and its application for semi-active control of vehicle suspension system*. Mechatronics, 2002 . 12(7): pp. 963–973

[2] Sharma, S. K., & Kumar, A.,*Ride comfort of a higher speed rail vehicle using a magnetorheological suspension system.* Proceedings of the Institution of Mechanical Engineers, Part K: Journal of Multi-Body Dynamics, 2018. 232(1): p. 32-48.

[3] Deng, Z., Wei, X., Li, X., Zhao, S., and Zhu, S. *Design and multi-objective optimization of magnetorheological damper considering vehicle riding comfort and operation stability*. Journal of Intelligent Material Systems and Structures, 2022. 33(9): p. 1215-1228.

[4] Zeng, W., Jiang, Q., Liu, Y., Yan, S., Zhang, G., Yu, T., and Xie, J. *Core power control of a space nuclear reactor based on a nonlinear model and fuzzy-PID controller*. Progress in Nuclear Energy, 2021. 132: p. 103564.

[5] Mitra, P., Dey, C., and Mudi, R. K. *Fuzzy rule-based set point weighting for fuzzy PID controller*. SN Applied Sciences, 2021. 3(6): p. 651.

[6] Bai, R., and Wang, H. B. *Robust optimal control for the vehicle suspension system with uncertainties*. IEEE transactions on cybernetics, 2021. 52(9): p. 9263-9273.

[7] Zhang, R., Zhao, L., Qiu, X., Zhang, H., and Wang, X. *A comprehensive comparison of the vehicle vibration energy harvesting abilities of the regenerative shock absorbers predicted by the quarter, half and full vehicle suspension system models*. Applied Energy, 2020. 272: p. 115180.

[8] Yang, C., Xia, J., Park, J. H., Shen, H., and Wang, J. *Sliding mode control for uncertain active vehicle suspension systems: an event-triggered H∞ control scheme*. Nonlinear Dynamics, 2021. 103(4): p. 3209-3221.

[9] Liu, L., Zhu, C., Liu, Y. J., and Tong, S. *Intelligent motion tracking control of vehicle suspension systems with constraints via neural performance analysis*. IEEE Transactions on Intelligent Transportation Systems, 2021. 23(8): p. 13896-13903.
[10] Emam, A. S. *Fuzzy Self Tuning of PID Controller for Active Suspension System*. Advances in Powertrains and Automotives, 2015.1(1): pp. 34-41
[11] Zhu, H., Rui, X., Yang, F., Zhu, W., and Wei, M. (2019). *An efficient parameters identification method of normalized Bouc-Wen model for MR damper*. Journal of Sound and Vibration, 2019. 448: pp. 146-158.
[12] Niola, V., Palli, G., Strano, S., and Terzo, M. *Nonlinear estimation of the Bouc-Wen model with parameter boundaries: Application to seismic isolators*. Computers & Structures, 2019. 222: p.1-9.
[13] Pelliciari, M., Marano, G. C., Cuoghi, T., Briseghella, B., Lavorato, D., and Tarantino, A. M. *Parameter identification of degrading and pinched hysteretic systems using a modified Bouc–Wen model*. Structure and Infrastructure Engineering, 2018.14(12): p. 1573-1585.
[14] Hu, G., Liu, Q., Ding, R., and Li, G.*Vibration control of semi-active suspension system with magnetorheological damper based on hyperbolic tangent model*. Advances in Mechanical Engineering, 2017. 9(5): pp. 1687814017694581.